13. MICROSTRUCTURAL ANALYSIS OF SITES 891 AND 892: IMPLICATIONS FOR DEFORMATION PROCESSES AT THE FRONTAL THRUST AND AN OUT-OF-SEQUENCE THRUST[1]

Philip A. Teas,[2] Harold J. Tobin,[2] and Pilar E. García[3]

ABSTRACT

Microstructures preserved in cores recovered from the Cascadia accretionary wedge during Ocean Drilling Program Leg 146 provide direct insight into the current structural processes active in the wedge. Sediment in the hanging wall of the frontal thrust at Site 891 is laterally shortened by mild deformation features. The upper frontal thrust splay at 375 mbsf exhibits collapse features associated with fault normal compaction and has well-developed fabrics which suggest relatively large strain accommodation. Dilational, plastic deformation, and less strain indicated by microstructures from the middle splay at 426 mbsf are inferred to be a result of high pore pressure during deformation. Between the middle and lower frontal thrust splays, sediments exhibit no tectonic strain.

At Site 892, normally to overconsolidated material initially dilated with shearing, producing isolated blocks of sediment that behave as coherent clasts within the deforming material. Bulk ductile deformation of unlithified sediment is indicated in the hanging wall of the out-of-sequence thrust by a penetrative high-conjugate-angle set of foliations. Microfabric intensity increases with proximity to the out-of-sequence thrust reaching a maximum within the fault zone. Horizontal extension in the hanging wall is shown by displacement indicators and is attributed to anticlinal folding above the thrust. Calcite precipitation in a shear zone within the hanging wall may indicate high pore-pressure events synchronous with deformation. The out-of-sequence thrust zone, identified by the Leg 146 Shipboard Scientific Party, has highly variable microstructures. An interval of intense deformation at 105–110 mbsf indicates high strain; otherwise, the material is deformed to the same degree as the hanging wall. Calcite veins present near the top of the fault zone indicate fluid flow associated with faulting. Concentrated deformation has led to highly overconsolidated material; however, plastic deformation is indicated throughout and high pore pressures during deformation are inferred.

INTRODUCTION

The large-scale framework of deformation occurring in accretionary wedges is well understood. However, in order to more fully understand the deformation mechanisms active during accretion it is critical to examine structures directly at core and microscopic scales. The fundamentals of wedge deformation are primarily determined from field mapping (Bally et al., 1966; Roeder et al., 1978), seismic reflection surveys (von Huene, 1979; Aoki et al., 1982; White and Louden, 1983), and critical taper models relying on the overall geometry of wedges (Davis et al.,1983; Dahlen, 1990). The hydrologic regime of the wedge strongly influences the structural style (Hubbert and Rubey, 1959; Moore and Vrolijk, 1992), and a great deal of current work is focusing on determining the interrelationship of hydrologic characteristics and deformation. Microstructural analysis is a means of observing features which record deformation and provide indications for the active processes and style of deformation occurring at various locations in the wedge. Microstructures can therefore constrain proposed deformation mechanisms and indicate the importance of various factors influencing deformation, including the role of fluids.

Analysis of accretionary wedge microstructures has been relatively limited, primarily because of scarcity of samples and difficulty in working with unlithified sediment. Examples of microstructures from active accretionary wedges were compiled by Lundberg and Moore (1986). Here we document and interpret microstructures developed at Sites 891 and 892 in the toe of the Cascadia accretionary wedge, using the descriptive and analytical framework of Knipe (1986), Carson and Berglund (1986), Arch et al. (1988), and Maltman et al. (1993). In addition, we interpret microstructures with respect to their position in the wedge providing constraints on contrasting deformation mechanisms active in various locations.

Leg 146 provides an excellent opportunity to examine microstructural variation and to correlate microstructures to the large-scale structure and hydrologic regime of this accretionary wedge. Sites 891 and 892 are of primary interest, as they allow study of two very different structurally active regimes. Drilling at Site 891 penetrated newly accreted sediment faulted by two splays of the frontal thrust. Site 892 penetrated normally to overconsolidated sediment with a generally high degree of deformation and a longer history within the wedge faulted by an active out-of-sequence thrust.

The frontal thrust and the out-of-sequence thrust are known to be structurally and hydrologically active (Moore et al., 1991; Westbrook, Carson, Musgrave, et al., 1994). Negative polarity reflectors on the frontal thrust, seen in seismic reflection data, are interpreted as areas of high pore pressures (Moore et al., in press). Pore-water chemistry anomalies from both sites are concluded to be a result of advection of fluids along faults (Westbrook, Carson, Musgrave, et al., 1994). The out-of-sequence thrust is associated with a pull-up of the bottom-simulating reflector, believed to be a result of advection of relatively warm fluids along the fault (Moore et al., 1991). Additionally, cold seep communities present at the intersection of the seafloor and both the frontal thrust and out-of-sequence thrust indicate fluid flow (Moore et al., 1991).

METHODS

Intervals of whole-round cores and other intact samples were collected from geographically unoriented cores aboard ship and sealed

[1]Carson, B., Westbrook, G.K., Musgrave, R.J., and Suess, E. (Eds.), 1995. *Proc. ODP, Sci. Results,* 146 (Pt. 1): College Station, TX (Ocean Drilling Program).

[2]Earth Science Board, University of California, Santa Cruz, CA 95064, U.S.A.
[3]Department of Geological and Environmental Sciences, Stanford University, Stanford, CA 94305, U.S.A.

to preserve original pore fluids. Sample collection from areas of cores lacking macroscopic drilling deformation minimized the occurrence of drilling-related features in thin section. Despite these precautions, examples of drilling deformation were found. These features are omitted from descriptions and have been considered when describing other structural features in slides in which they occur. Thin section preparation followed Grimm's (1992) technique of stepped replacement of pore fluid with acetone and low-viscosity SPURR resin, following recommendations in Jim (1985) and Swartz and Lindsley-Griffin (1990). Each sample was cut into two mutually perpendicular sections parallel to the core axis, to permit three-dimensional analysis of structures.

Most of the geometric characterization of microstructures is from optical microscopy. The degree of parallel alignment of phyllosilicates was qualitatively established by viewing thin sections between crossed polars with a quartz plate inserted. Optical axes of phyllosilicates are aligned parallel to crystallographic axes, so parallel phyllosilicates have coincident optical axes and become extinct at the same degree of stage rotation. The intensity of colors in optical microscopy corresponds to the intensity of grain alignment (Morgenstern and Tchalenko, 1967). Scanning electron microscopy (SEM) of broken, air-dried samples was used to image grain fabrics at a finer scale. Additionally, ten of the samples were chosen for cathodoluminescence imaging to determine the importance of calcite cementation.

We quantified observations of "residual clasts" found in sediments from Site 892 by measuring area and aspect ratio and qualitatively analyzing roundness. We recorded residual clasts, in thin section, on videotape and transferred video frames into NIH Image analysis software. Clast measurements from each thin section for a given sample were averaged to obtain a representative value for the sample.

MICROSTRUCTURES

Microstructures observed in Cascadia wedge sediments largely fall into the classification scheme of the Maltman et al. (1993) for Nankai wedge sediments. We provide brief descriptions following their scheme and describe other structural fabrics that do not fit well into their categories. The sediments collected are primarily clayey silts with infrequent sand and clay layers and abundant siliceous microfossils. The irregular shapes and large grain size of microfossils contribute to poor alignment of grains and affect the appearance of microstructures.

Bedding Fabric

Bedding orientation is discernible only in a few samples that contain either turbidite deposits or isolated sand or clay layers. Where bedding is recognizable, a preferred orientation of phyllosilicates and elongate grains parallel to the bedding orientation is almost always noted. This fabric is a result of uniaxial compression associated with burial, and generally is more intensely developed with depth. Many samples that lack bedding indicators also have a preferred orientation of phyllosilicates and elongate grains; because bedding is not recognized it is not possible to determine whether the fabric is a result of compression due to burial or tectonism. Throughout this paper we refer to these fabrics as compaction fabrics, noting bedding when present.

Deformation Bands

Deformation bands refer to any discrete planar or curviplanar structural features noted in samples. This covers a wide range of appearance of structures, each a result of deformation concentrated in a narrow zone producing some degree of displacement.

Kink Bands

Deformation bands with an internal fabric of grains aligned at an angle to the trend of the band and up to 90° to the compaction fabric are consistent with previous description of kink bands (Lundberg and Moore, 1986; Maltman et al., 1993). Kink bands are narrow (0.04–0.1 mm in width), have distinct boundaries in clay-rich layers, but are broad with indistinct boundaries in sands. Deflection of the external grain fabric occurs across a narrow zone at the kink boundaries and the acute angle between the kink band orientation and grains within the kink band points in the direction of displacement. Although both normal and reverse displacement indicators are found in Cascadia samples, reverse displacement is dominant. Kink bands are present in few samples, generally only where deformation is mild.

Shear Zones

Deformation bands with a complex internal structure of subsidiary shear bands are common in Cascadia wedge samples. The subsidiary structure resembles Riedel shear structure described in shear zones by previous authors (Morgenstern and Tchalenko, 1967; Logan et al., 1979; and Maltman et al., 1993). Figure 1 illustrates the orientation and nomenclature modified from Logan et al. (1979) used to describe subsidiary shear bands. All subsidiary shear band orientations are not developed in any one shear zone. Subsidiary shear bands are defined by narrow bands of elongate grains aligned parallel to the orientation of the subsidiary band. Grain size is often finer in the subsidiary shear bands than in the matrix; however, no evidence for cataclasis is seen and grain-size reduction is thought to be due to disaggregation of clay minerals. Deformation is accommodated by independent particulate flow; grains slide against each other without breakage. Subsidiary thrust or P-shear bands are relatively common in Cascadia samples though generally less common than R-shears in the literature. Subsidiary Y-shear bands developed parallel to the shear zone indicate significant strain (Mandl, 1977; Logan et al., 1979). Shear zones often, but not always, are bounded on one or both sides by subsidiary Y-shear bands. The material within shear zones between subsidiary shear bands usually has a preferred orientation which will be referred to as the shear zone matrix fabric. In some cases, the shear zone matrix fabric is oriented parallel to a compaction fabric outside the shear zone, but more commonly the orientation is independent of other fabrics. The orientations of the subsidiary shear bands depends on the orientation of the stress field within the shear zone and the properties of the shear zone material during deformation.

Single-strand Shear Zones

An additional type of deformation band present in Cascadia samples is intermediate between the kink band and shear zone classifica-

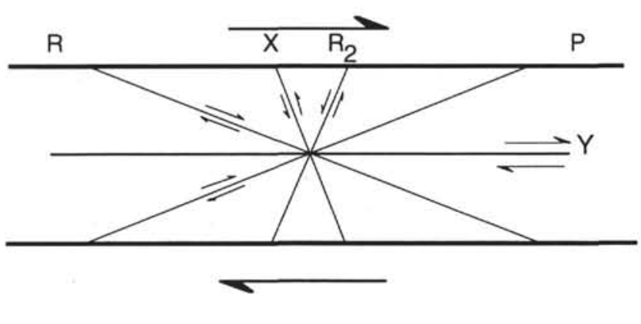

Figure 1. Geometry of subsidiary shears relative to a right lateral shear zone. Angles are approximated for a plastic shear zone. Modified from Logan et al. (1979).

tion. Similar to kink bands, these bands occur as spaced sets of planar to anastomosing narrow bands, but grains are aligned parallel to the band orientation, resembling subsidiary shear bands in shear zones. Unlike shear zones they have no internal subsidiary structure, yet bedding is clearly offset across bands in many samples. Offsets of 0.01–2.0 mm occur across these bands, with the highest offset occurring on the widest bands. Band width varies between <0.01 and 0.08 mm. Spacing between bands varies from 0.02 to 1.5 mm. The anastomosing pattern of closely spaced sets of bands often approximates Riedel orientations.

Distributed Conjugate Fabric

Many samples from Site 892 are characterized by two interpenetrating fabrics. Each fabric forms broad areas with preferred orientation of clays and phyllosilicates. Under high magnification the fabrics are shown to be interpenetrative on the grain scale which indicates synchronous formation and a conjugate fabric relationship. The dips of these fabrics vary from 6° to 85° but are consistent to within ±10° in any individual sample. The conjugate angle ranges from 38° to 90°, but is typically 80°–90°; one fabric gently dipping, the other steeply dipping. Clay layers sheared along both distributed conjugate fabrics provide displacement direction indicators consistent with horizontal extension and vertical compression.

Residual Clasts

Undeformed bodies of clayey silt, compositionally and texturally similar to the surrounding matrix, are common throughout samples from Site 892. Cathodoluminescence indicates no preferential carbonate cementation of these clasts relative to the surrounding matrix; however, authigenic clay cements have not been ruled out. It is clear that formation is in situ because of the similarity of composition between the clast and the surrounding material.

Site 891: Frontal Thrust

Macroscopic examination of the 470-m cored interval identified five structural domains and two major faults at 263 and 375 meters below seafloor (mbsf), corresponding to splays of the frontal thrust (Shipboard Scientific Party, 1994a). Moore et al. (this volume) identify three splays on the basis of seismic reflection data at about 375, 426, and 500 mbsf. Microstructural analysis of samples from Hole 891B allows characterization of various structural features in domains II, IV, and V (Fig. 2). Hanging wall samples show only minor deformation, whereas samples from the frontal thrust zone display a wide variety of deformational features, from undeformed between splays, to compacted and dilated material associated with the upper and middle frontal thrust splays, respectively.

Hanging Wall

Hanging wall samples contain moderately dipping clayey silts and fine sands, interpreted as distal turbidites. A moderate compaction fabric developed parallel to bedding prior to folding. Narrow bedding-parallel shear zones, 0.2–0.4 mm wide, within the upper, finest clay-size material of several turbidite sequences indicate strain partitioning within finest grain-size layers (Pl. 1, Fig. 1). These shear zones are bounded by well-developed Y-shears at the base and become indistinct upward into sand-size sediment. Spaced low-angle subsidiary shears of P- or R-geometry are poorly developed. Displacement direction is indeterminate, but if thrusting is assumed, the subsidiary shears are P-shears. The orientation of the shear zone matrix fabric at a high angle to both the subsidiary shears and the compaction fabric outside the shear zone indicate widening of the band and lateral shortening. Reorientation of all material within the shear zones indicates ductile deformation.

Kink bands occur in a wide range of orientations within a single thin section, dipping 21°–82°, and consistently indicate reverse displacement. Kink bands are planar to slightly anastomosing with indistinct boundaries and vary in width from 0.04 to 0.1 mm. They are most distinct in clay-rich layers and either terminate or become broad and indistinct as they pass through sands. Mutual cross-cutting relationships between kink bands and shear zones indicate synchronous formation. Kinks are often bounded by fractures in thin section and may cause the slightly polished fractures seen in cores (Shipboard Scientific Party, 1994a).

Frontal Thrust: 375-mbsf Splay

We collected two samples from the vicinity of the upper thrust splay. The first sample, from Section 146-891B-47X-2 at 366 mbsf, shows an abrupt transition from sediment with a weak, steeply dipping compaction fabric into a well-developed, subhorizontal shear zone at least 4 mm wide with unknown sense of displacement. Two grain fabric orientations are evident in this shear zone: a distributed alignment parallel to the shear zone with rare distinct Y-shears (Pl. 1, Fig. 2) and discontinuous, narrow, poorly defined subsidiary bands at an angle of about 12° to the shear zone (Pl. 1, Fig. 3). The classification of these subsidiary bands is unclear, as displacement sense is unknown. Locally, a fabric with similar dip to the compaction fabric above the shear zone is present between subsidiary bands. Electron microscopy reveals an essentially planar fabric of strongly aligned platy grains (Pl. 1, Fig. 4), which we interpret as the shear zone parallel fabric. This sheet structure is anastomosing in SEM images due to the intersection of the Y-fabric with the low-angle subsidiary bands and heterogeneous grain size.

The second sample, from Section 146-891B-48X-1 at 375 mbsf, contains an extremely well-developed fabric defined by very strong alignment of phyllosilicates dipping 31°. Convolutely folded sand layers are slightly offset across the fabric, but discrete deformation bands are not developed. This fabric represents distributed simple shear along planes parallel to a compaction fabric formed after folding. A subhorizontal shear zone, 0.4 mm wide, with a geometry similar to those in the hanging wall, cuts across the fabric with reverse displacement, offsetting a sand layer 3.4 mm. The orientation of subsidiary shear bands is consistent with P-shears.

Frontal Thrust: 440-mbsf Splay

Recovered material shows reduced evidence of deformation between 375 and 438 mbsf, where macroscopic deformation bands were reported (Shipboard ScientificParty, 1994a). The restricted nature of these bands may be a result of poor core recovery, and a major fault may be nearby and unsampled. The deformation features in the recovered Sample 146-891B-55X-2, 74–85 cm, is quite different from those described above. Shear zones 1–3 mm wide are spaced approximately 5 mm apart, dip 6°–11° at a high angle to the nearly vertical bedding and bedding parallel compaction fabric, indicate reverse displacement, and have complex internal structure (Pl. 2, Figs. 1 and 2). Offset across the shear zones is of the same order as the width of the shear zone. Shear-zone-parallel distributed alignment of phyllosilicates is the dominant grain orientation within the shear zone (Pl. 2, Fig. 1), but is weakly developed relative to the 366 mbsf sample. Well-developed, slightly sigmoidal, subsidiary P-shears are oriented at 45° to the band orientation (Pl. 2, Fig. 2). Moderately well-developed shears dip 48°–60° opposite the P-shears and form a conjugate angle of 75°–87°. Within the shear zone, between an offset sand layer, there is no increase in volume of sand grains. Cataclasis is not indicated and flow of material in the shear zone is inferred.

Near the bottom of the hole at 464 mbsf, between the middle and lower thrust splays, subhorizontally bedded turbidite sequences are present but lack visible deformation features (Pl. 2, Fig. 3). Relative-

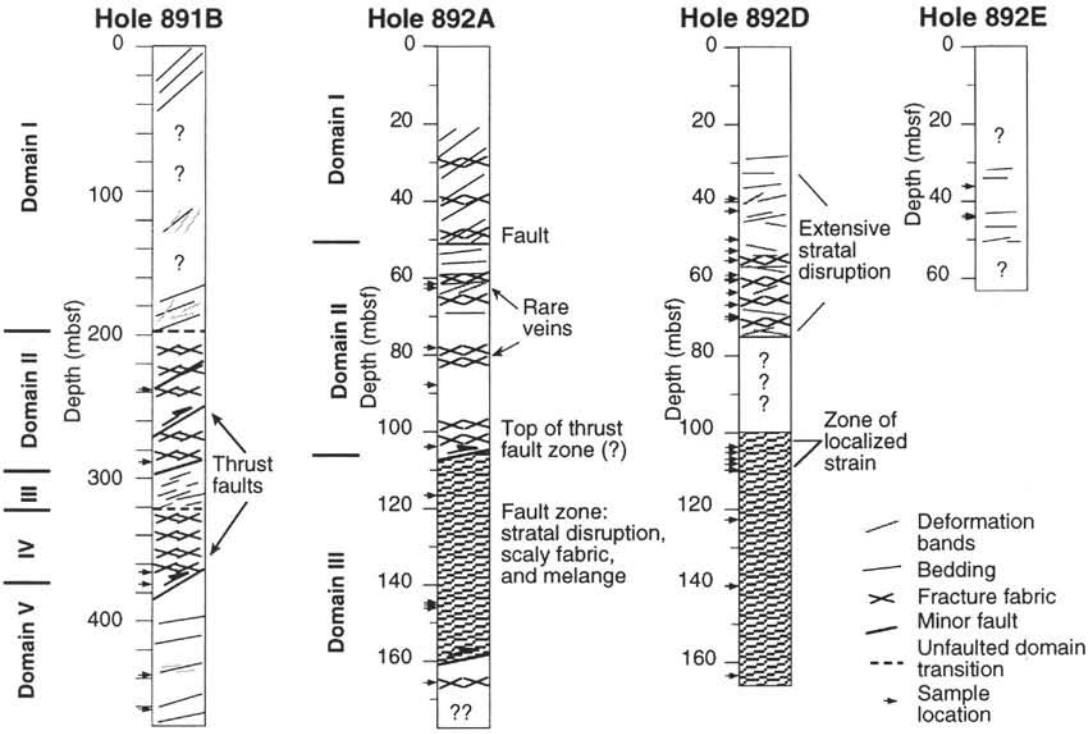

Figure 2. Summary diagram of structural features of Sites 891 and 892 showing positions of samples studied for this paper. Modified from Westbrook, Carson, Musgrave, et al. (1994).

ly weakly developed bedding-parallel orientation of elongate grains indicates a relatively small degree of gravitational compaction compared to sediment in the hanging wall.

Site 892: Out-of-Sequence Thrust

Improved core recovery at Site 892 resulted in greater sample coverage and more complete characterization of structures. We collected samples from Holes 892A, 892D, and 892E, to allow comparison of structures between holes (Fig. 2). Shipboard macroscopic examination identified three structural domains and two faults at 52 and 105–150 mbsf (Fig. 2) (Shipboard Scientific Party, 1994b). The shallow 52 mbsf fault is only found in Hole 892A and is above the shallowest sample from that hole. Microstructural evidence suggests that the deeper fault, believed to be the out-of-sequence thrust imaged in seismic data, is actually on the order of several meters wide at approximately 105 mbsf in Hole 892D. Evidence for a third fault is found at approximately 66 mbsf in Hole 892D.

Hanging Wall

Comparison of samples from Holes 892E, cored by advanced piston coring, and Hole 892D, cored by extended core barrel, which induces rotational torque on the cores, reveals similar structures at shallow depths and no additional features attributable to drilling deformation. The shallow samples are clayey silts with abundant whole and fragmented diatoms and radiolarians of Pliocene age.

Several samples exhibit both a gently dipping compaction fabric with discrete fabric-parallel single strand shear zones, and steeply dipping kink bands in a mutually cross-cutting relationship (Pl. 3, Fig. 1). More commonly, samples contain a distributed conjugate fabric with discrete fabric-parallel, spaced sets of single strand shear zones in both conjugate orientations (Pl. 3, Figs. 2 and 3). The gently dipping shear zones are more extensively developed and more commonly truncate the steeply dipping shear zones. Kink bands are occasionally present parallel to the steeply dipping conjugate fabric.

SEM images from the hanging wall show both essentially planar fabrics of aligned phyllosilicates and areas of randomly oriented grains (Pl. 3, Fig. 4). The grains that comprise the planar features, interpreted as single-strand shear zone surfaces, are not strongly aligned. The second primary fabric occurs as a subtle spaced cleavage (Pl. 3, Fig. 4).

With increasing depth to 63 mbsf in Hole 892D and from 61 to 62 mbsf in Hole 892A, samples show a trend toward stronger development of conjugate fabrics. Samples are consistently composed of clayey silt with abundant whole and fragmented silicate microfossils. Areas of distributed conjugate fabrics become smaller as single strand shear zones in both orientations become more numerous, better defined, more continuous, and more closely spaced. The gently dipping shear zones generally are more continuous and better developed, with narrower bands of more strongly aligned grains. These shear zones vary in style from single wide bands to networks of closely spaced anastomosing narrow bands separated by material oriented parallel to the conjugate fabric. Offset is greatest across the most well-developed shear zones.

Samples from Sections 146-892D-5X-4 and 6X-3 at depths of 42 and 50 mbsf contain abundant detrital carbonate grains averaging 0.01 mm in diameter. Within shear zones, the distribution is reduced locally by as much as 80%. The shear zones appear to be areas of enhanced dissolution of calcite due to either fluid flow and/or pressure solution. Abundant glauconite pellets in these two samples and from Section 146-892D-7X-5 show various effects of deformation (Pl. 4, Fig. 1). Nonspherical pellets tend to have long axes aligned parallel to the compaction fabric, and pellet edges are often flattened parallel to the grain fabrics. Pellets are often cut by or stretched out within the shear zones. Within wide continuous bands, reduction of pellet size and more angular pellet shapes indicate cataclasis.

Discontinuous, steeply dipping planar kink bands occur in relatively highly deformed samples from Sections 146-892A-8X-3 and 8X-4 and Sections 892D-7X-5 and 8X-2. Kink bands occasionally cut across the above fabrics, but more often terminate into them, generally with no clear offset counterpart noted across the truncating shear zone. Both reverse and normal displacement are indicated across kink bands.

Minor Fault Zone: 66 mbsf

A sample from Section 146-892D-8X-CC collected at 66.7 mbsf contains several large clasts ranging from 1 mm to 2 cm in diameter. Phyllosilicates within the clayey silt matrix are randomly oriented except where relative motion between adjacent clasts has caused localized shear. One type of clast is composed primarily of large equidimensional calcite crystals up to 2 mm in diameter. Quartz and feldspar sand grains adjacent to the areas of large crystals are fractured and cemented with calcite. One clast contains two bands of oriented, elongate calcite crystals and mud stringers separated by a band of large equidimensional calcite crystals (Pl. 4, Fig. 2). These bands indicate shearing of the matrix synchronous with dilation and calcite precipitation. The bands of equidimensional calcite crystals are interpreted to have grown within large open fractures. Sheared mud incorporated within these crystals indicates that crystal growth occurred after the shearing event (Pl. 4, Fig. 2). Inclusions of blebs and stringers of mud within some crystals (Pl. 4, Fig. 2) must have broken off of the fracture walls and been incorporated into the growing crystals.

The second type of clast is composed of sand grains and clayey silt with calcite cement. Many sand grains have internal calcite veins which do not extend beyond the grain boundary (Pl. 4, Fig. 3). This structure is formed by brittle fragmentation within the fault zone followed immediately by precipitation of cement. Cataclasis may be enhanced in this area as cementation increases the strength of the sediment.

Samples with strongly developed fabrics were collected between faults from Section 146-892D-9X-1 at 69.5 and 70.3 mbsf and from Sections 146-892A-11X-1, 12X-1, and 13X-8 at 78, 87.9, and 103.8 mbsf. Three fabrics are present: a conjugate set similar to those described above; a well-developed fabric roughly bisects the conjugate set (Pl. 5, Figs. 1 and 2); and a third fabric overprints the conjugate set, forming broad areas of simultaneous extinction and rare distinct single strand shear zones (Pl. 5, Fig. 1). Well-developed wide deformation bands, viewed at higher magnification, are composed of a network of very closely spaced narrow bands (Pl. 5, Fig. 3).

Out-of-Sequence Thrust Zone: 105–110 mbsf

Microstructures within the out-of-sequence thrust are highly variable, partially in response to changing lithology. At the top of the fault zone, a sample from Section 146-892D-10X-3 contains three fabrics similar to those above the fault. A clay layer sheared along the conjugate fabrics indicates displacement of about 0.08 mm and extension parallel to the third fabric that dips 16° and roughly bisects the conjugate set. Long axes of residual clasts are preferentially aligned parallel to the third fabric, which occurs as distributed alignment of grains with only few discrete bands. Crystalline calcite present in thin section occurs in several forms: large clasts, up to 5 mm in diameter, of fragmented carbonate mud cemented by large calcite crystals; fragments of single crystals; a calcite infilled foraminifer test; and veins within residual clasts (Pl. 5, Fig. 5).

SEM images show an open framework of weakly aligned phyllosilicates (Pl. 5, Fig. 4). Single strand shear zones appear as parallel, spaced, planar surfaces composed of strongly aligned micron-scale grains that are laterally discontinuous and truncate in areas of grains oriented essentially perpendicular to the surface.

Sample 146-892D-10X-4, 124–128 cm, from 105.0 mbsf is the most highly deformed sample collected. No microfossils are present and grain size is relatively fine. The sample is deformed by four interpenetrating fabrics. The dominant fabric, dipping 37°, is defined macroscopically as a melange fabric (Shipboard ScientificParty, 1994b). In thin section, it occurs as very strong parallel alignment of phyllosilicates forming both continuous very closely spaced, narrow, anastomosing single-strand shear zones and distributed zones of aligned grains (Pl. 6, Figs. 1 and 2). Long axes of residual clasts are preferentially oriented parallel to this fabric.

Two fabrics are evident at 47°–53° to either side of the dominant fabric (Pl. 6, Figs. 3 and 4). They are equally well developed, discontinuous, planar to anastomosing single-strand shear zones. The fabrics are mutually cross-cutting and interpenetrating. The fourth fabric occurs as short bands of aligned grains approximately perpendicular to the dominant fabric. Though typically discontinuous and truncated by the dominant fabric, a mutual cross-cutting relationship exists.

Some of the abundant residual clasts in this sample are offset and provide shear sense indicators. Clasts show a wide range of behavior from intact rounded clasts, to flat-edged clasts thought to be recently sheared but lacking an offset portion, to clasts cut by a shear zone with some displacement evident. Motion along the dominant 37° fabric is consistent with thrusting (Pl. 6, Fig. 5). The two fabrics at about 45° to the dominant fabric have good shear sense indicators with a conjugate relationship indicating extension parallel to the dominant fabric (Pl. 6, Fig. 5).

Single-strand shear zone surfaces in SEM consist of essentially planar sheets of strongly aligned grains down to micron scale (Pl. 6, Fig. 6). Though parallel alignment is good, fabrics are not penetrative. The overall fabric remains fairly open, containing areas of variably oriented grains between parallel shear zone surfaces as a result of the well-developed complex interpenetrating fabrics.

This style of deformation continues with depth in Sections 146-892D-10X-6, 10X-7, and 10X-8. The dominant fabric changes dip from 37° to 66°, suggesting folding, rotation due to variable total strain, or reorientation of stress between samples. All fabrics are increasingly less well developed with depth (Pl. 7, Figs. 1 and 2), becoming more discontinuous, narrower, and less well defined. The angular relationship between fabrics remains the same as in the more highly deformed samples above. Similar fabrics are also present in Hole 892A in Section 18X-1 at a depth of 145 mbsf, but are relatively weakly developed.

Foot Wall

Below the zone of localized strain, samples exhibit deformation features similar to those in the hanging wall. The variation in style of fabrics is poorly constrained and no obvious trends in development are noted. The overall intensity of deformation is less than in samples from the hanging wall just above the top of the fault.

Residual Clasts

Few clasts are present in the upper portion of the hanging wall; however, clast size is at a maximum (Fig. 3). The number of clasts increases dramatically within the out-of-sequence thrust from less than 10 clasts to greater than 70 clasts per sample (Fig. 3A). The number of clasts is actually much greater in the fault zone due to the presence small clasts too numerous to count. Clast area is increased within the relatively less deformed underthrust material in Hole 892D (Fig. 3C), whereas Hole892A shows a decrease below the fault zone. We also notice a marked decrease in roundness of clasts within the fault zone due to the breakup of large clasts along planes, producing angular fragments; the smaller clasts are generally well rounded. The increased number of clasts and reduced average size in the fault zone relative to the upper hanging wall and footwall supports the evidence of clast breakup in the fault zone. The lack of shear fabrics within the clasts indicates clast formation prior to fault related deformation.

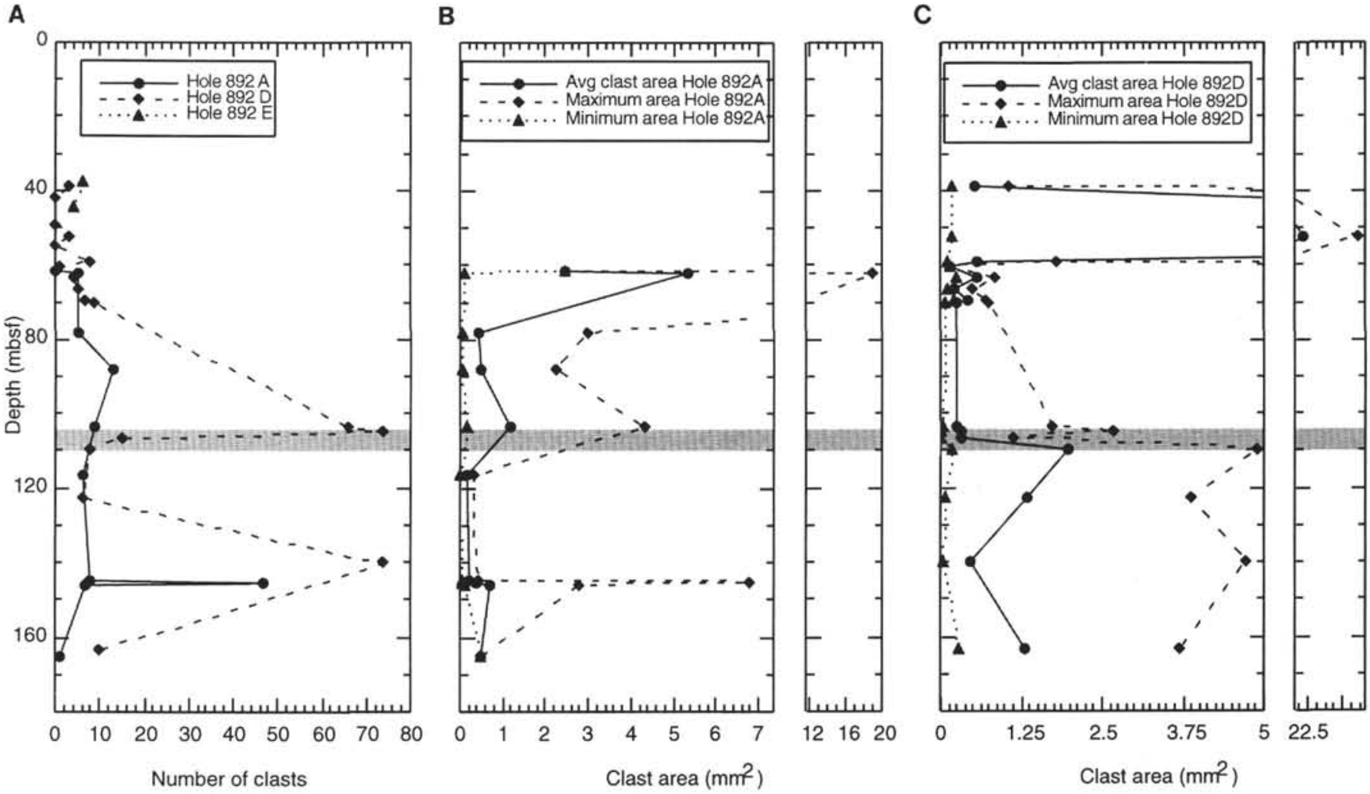

Figure 3. **A.** Number of residual clasts vs. depth at Site 892. Residual clast areas vs. depth for Hole 892A (**B**) and 892D (**C**). Gray bar indicates location of out-of-sequence thrust in Hole 892D.

SUMMARY

Site 891

At Site 891 microscopic examination supports the macroscopic observation of a general increase in deformation with depth within the hanging wall of the frontal thrust.

Compaction fabrics present within each sample generally increase in degree of alignment with depth. Where bedding orientation can be determined, bedding-parallel-orientations indicate compaction prior to folding. The weak compaction fabric in sediment between the middle and lower frontal thrust splays suggests relatively less compaction than in the hanging wall.

Kink bands, common in the hanging wall, occur over a wide range of orientations. They develop synchronously with minor low-angle shear zones and consistently accommodate reverse displacement. Shear zones form discrete narrow bands with subsidiary shears indicative of P-shears. The shear zones indicate ductile deformation, widening of shear zones during deformation and strain partitioning within fine clay-size material. Limited recovery precludes interpretation of trends in the geometry of shears within the hanging wall.

Two splays of the frontal thrust were sampled at 375 and 440 mbsf. High strain and compaction normal to shear zones are indicated in thin section and SEM along the 375-mbsf splay. The deformation bands correlated to the 440-mbsf splay contain a complex set of subsidiary shears indicating ductile deformation and flow of material in the deformation bands.

Site 892

Microstructural fabrics show an overall trend of increasing intensity and complexity of deformation with depth and proximity to the out-of-sequence thrust. Within the upper hanging wall two fabrics are present, a compaction fabric with discontinuous single strand shear zones parallel to the compaction fabric, and either steeply dipping kink bands or single-strand shear zones. Single-strand shear zones dominate sections with a higher degree of deformation.

The variation in degree of alignment of grains parallel to the compaction fabric is heterogeneous with depth and cannot be entirely attributed to gravitational loading. In many samples, displacement on the order of tens of microns occurs along the compaction fabric without development of discrete deformation bands. Such distributed minor offset enhances fabric-parallel grain alignment.

Distributed conjugate fabrics dominate microstructures in the hanging wall. Discrete single-strand shear zones parallel to the distributed fabric orientations are developed with increasing depth. The two fabrics commonly have a high conjugate angle and are not developed equally, with gently dipping orientations preferred. Single-strand shear zones first occur as relatively widely spaced discontinuous bands of weakly aligned phyllosilicates. With depth they are more closely spaced and better defined with sharper boundaries and more strongly aligned grains. Areas of distributed fabrics are reduced in samples with more, discrete continuous shear zones. With proximity to the main fault zone a subhorizontal fabric, forming broad areas of preferred grain alignment with rare discrete bands, overprints the conjugate set, bisecting the conjugate angle.

The four interpenetrating fabrics present within the out-of-sequence thrust zone vary in intensity with depth. The dominant melange fabric becomes more steeply dipping with the other fabrics maintaining their relative orientations. All fabrics are less well developed with depth but maintain their relative magnitudes. Displacement indicators show reverse displacement on the dominant fabric and extension parallel to the dominant fabric due to conjugate displacement on the equally well-developed fabrics at 45° to either side of the dominant fabric.

Below the out-of-sequence thrust (an intense zone of deformation between 105 and 110 mbsf in Hole 892D) sediment is less deformed than in the hanging wall directly above the fault zone. Samples from the footwall exhibit varying features, from distributed conjugate fabrics with fabric-parallel single-strand shear zones to conjugate fabrics overprinted by a third, bisecting fabric.

MICROSTRUCTURE GEOMETRY: IMPLICATIONS FOR STYLES OF DEFORMATION

Frontal Thrust: 375-mbsf Splay

Closely spaced subsidiary bands at a low-angle to the trend of the deformation band may represent either Riedel or P-shears (Pl. 1, Fig. 3). The displacement direction is not indicated in thin section; however, if thrust faulting is assumed then the subsidiary bands are P-shears. Formation of P-shears requires principal stress orientation at an acute angle to the shear zone. Poor band-parallel alignment of phyllosilicates and indistinct boundaries of P-shears are attributed to very small displacement on any individual band. Displacement on subsidiary P-shears leads to widening of the deformation band, in conflict with compaction indicated by the Y-shear fabric, so we infer that closely spaced P-shears develop due to arrested motion on any individual P-shear band.

The strong fabric developed parallel to the orientation of the shear zone (Pl. 1, Fig. 2) is consistent in orientation with Y-shear fabric; however, discrete Y-bands are rare. Y-fractures are dominant in brittle shear zones where large amounts of displacement have occurred, (Mandl et al., 1977; Logan et al., 1979). Shear box experiments on clay also show the development of Y-shears with increasing strain (Morgenstern and Tchalenko, 1967). While the discrete bands can be explained by large strain accommodation, the distributed alignment of grains parallel to the shear zone is not. Tchalenko (1968) notes that the orientation of the grain fabric in shear zones is approximately normal to the average direction of the major principal stress. The shear-zone-parallel fabric in the frontal thrust sample is interpreted to indicate rotation of the major principal stress during deformation to a final orientation normal to the shear zone. Reorientation of grains parallel to the shear zone, from an original orientation parallel to the steeply dipping compaction fabric outside the shear zone, indicates significant consolidation.

Frontal Thrust: 440-mbsf Splay

Although some compaction is indicated by subsidiary structures in shear zones associated with the middle thrust splay, dilation is also apparent. The distributed alignment of phyllosilicates parallel to the shear zone indicates compaction normal to the shear zone as in the upper splay; however, the fabric is not as strongly developed. Compaction normal to the shear zone is interpreted after shear zone formation, due to overprinting of the P- and X-shears by the Y-fabric.

Well-defined sigmoidal P-shears with 75°–87° conjugate X-shears indicate a passive limit state of deformation within a frictional-plastic material (Mandl, 1988, pp. 172–174), consistent with lateral shortening and fold and thrust deformation of accretionary wedges. Mohr-Coulomb failure criteria holds that conjugate shear fabrics are generated at an angle of $45° - \phi/2$, where ϕ is the internal angle of friction, to either side of the major principal stress axis. For a conjugate set of 75°, ϕ is 15°; for 87° conjugates, ϕ is 3°. When ϕ is 0° and conjugates form at 90°, the material is frictionless and deforms as a purely cohesive perfectly plastic material (Mandl, 1988, p. 172). The major principal stress axis must be oriented at 2°–8° to the deformation band in order to bisect the P- and X-shears and produce appropriate offset along the P-shears. The well-developed nature of the P-shears suggests widening of the shear zone during failure.

Conjugate Fabrics at Site 892

The dominant fabric outside of fault zones at Site 892 consists of two distributed grain fabrics with a high conjugate angle geometry. Shearing along these fabrics without the generation of discrete deformation bands, indicated in several samples by small offset of clay layers, indicates horizontal extension or vertical compression. The high angle of conjugates, up to 90°, indicates values of the internal angle of friction approaching 0° and bulk plastic deformation of the unlithified sediment.

In mildly deformed samples, single-strand shear zones are discontinuous and form widely spaced sets of narrow anastomosing bands that may be a result of initial distributed conjugate fabrics. Arch et al. (1988) show a correlation between deformation band geometry and the intersection angle between the deformation band and original fabric. When the angle is high, deformation bands form anastomosing networks of bands, whereas a low angle results in discrete single bands. As single strand shear zones form in Cascadia samples they encounter areas of fabric at nearly 90° to the band orientation and either stop or form spaced networks. Discrete through-going deformation bands become dominant as the band passes into areas of distributed fabric aligned parallel to the deformation band.

Out-of-Sequence Thrust

Samples from Sections 146-892D-10X-4 through 10X-8 are deformed by four synchronously developed, interpenetrating fabrics. The most intense fabric, parallel to the macroscopically described melange fabric, is interpreted as a Y-shear fabric. The strong development of discrete Y-shear bands indicates large strain accommodation. The weakly developed fabric approximately perpendicular to the Y-shear fabric has a mutual cross-cutting relationship with the Y-shear fabric and is considered to be its conjugate. The equally well-developed subsidiary shear bands approximately 45° to either side of the Y-shear fabric are considered as a second set of conjugates and have displacement indicators consistent with R- and R_2-subsidiary shear bands (Pl. 6, Fig. 5). The approximate 90° conjugate angle for each set indicates plastic deformation. Increasingly weaker development of all four fabrics in lower sections of Core 146-892D-10X indicates less strain with depth. However, consistent relative magnitudes of each fabric demonstrates that all strain is not accommodated by the Y-shear fabric once formed, and R- and R_2-shears continue to develop. The orientation of the bisectors of the conjugate sets, and therefore the expected orientation of the major principal stress axes responsible for each set, are at 45° and 90° to the Y-shear fabric. Synchronous formation of both conjugate sets may be a result of microheterogeneity in the stress field as a result of extension parallel to the shear zone associated with development of the Y-shear fabric. Alternately, temporal variation in normal stress acting on the fault zone, possibly as a result of fluctuating pore pressure, may cause intermittent formation of the two conjugate sets.

RESIDUAL CLASTS

Some clasts are bounded by single strand shear zones which conform to the clast boundaries (Pl. 7, Fig. 3). These samples suggest that the clasts could be formed by isolation of a patch of clay material by intersecting shear zones. In other samples deformation bands terminate at clast boundaries (Pl. 7, Fig. 4) or band spacing is too small to isolate the size clasts present, and we call on dilation to explain the formation of the clasts. Sediments at Site 892 are Pliocene in age, have been uplifted by thrusting along the out-of-sequence thrust, and are expected to be overconsolidated. Movement along shear zones and faults in overconsolidated sediment theoretically leads to initial dilation. Such expansion could cause fractures to open and isolate pockets of coherent clay material that become residual clasts. The dilation hypothesis seems more probable when we consider that even the few highly deformed areas of Site 891 lack residual clasts. The critical difference between sites is the initial condition of the sediment.

The increased number of clasts within the fault zone is probably a result of breakup of clasts during fault-related deformation. The large clast area in the footwall in Hole 892D relative to that in the highly deformed sediments within and above the fault suggests initial large clast formation followed by size reduction during deformation. Clast formation may also be favored near the fault zone where both high strain localization and fluid transport occur, thus producing a greater number of clasts.

Maltman et al. (1993) and Byrne et al. (1993) describe a hydraulic breccia from the Nankai accretionary wedge that appears to be the initial stage of clast formation, without disruption by further deformation. The breccia consists of angular clasts thought to be formed by dilation associated with high pore pressure. They note the similarity in texture between the matrix and the breccia fragments, which is true of matrix and residual clasts in our samples.

MICROFOSSILS AND DEFORMATION

Siliceous microfossils are abundant in most samples collected at Sites 891 and 892. Elongate microfossils are aligned parallel to the compaction fabric where it occurs. Where two distributed fabrics occur, microfossils are aligned parallel to both fabric orientations which indicates rotation of fossils along with the phyllosilicates. Microfossils are generally absent within deformation bands with the exception of some wide bands. Within deformation bands microfossils are broken and often appear to be dissolved due to enhanced fluid flow or pressure solution. The presence of the microfossils promotes anastomosing of bands around large whole radiolarians and diatoms. Single bands also often split around microfossils. The presence of whole microfossils within distributed fabrics is due to ductile deformation and lack of significant compaction normal to those fabrics. The absence of microfossils in residual clasts within the out-of-sequence thrust at Site 892 indicates that no fossils were present at the location of fault localization. Moore and Lundberg (1986) suggest that the coarser grain size caused by the presence of microfossils may inhibit the localization of deformation within fossil rich sediments.

CONCLUSIONS

Site 891

Deformation in the hanging wall at Site 891 indicates ductile thrusting along subhorizontal shear zones and reverse displacement along kink bands. Localized strain is partitioned within fine-grain-size material at the top of turbidite sequences. Both kink bands and shear zones indicate horizontal shortening and vertical thickening along discrete bands. The sediment is apparently undeformed outside of these deformation bands.

Physical properties data (Shipboard Scientific Party, 1994a) show a decrease in porosity and increase in bulk density at a corresponding depth to the upper frontal thrust splay. This data combined with thin section observation (Pl. 1, Figs. 2 and 3) and SEM images (Pl. 1, Fig. 4) indicate collapse of the upper frontal thrust splay. Compaction due to faulting is expected in this region due to the presence of underconsolidated material (Moore et al., 1991). The extremely strong alignment of grains is thought to be the result of rotation during shear zone development followed by compaction normal to the shear zone as the last stage of deformation. Such collapse may be due to a decrease in pore pressure following shear zone development.

The middle frontal thrust splay is associated with deformation bands having complex subsidiary structures that indicate plastic deformation. Well-developed P-shears suggest widening of the shear zones as well as lateral compression. The absence of sand grains within a wide shear zone between offset sand layers can be explained by two mechanisms. Dilation and flow of sediment into the shear zone is possible; however, no disturbance of the compaction fabric adjacent to the shear zone boundaries is noted, so that the source for the sediment within the shear zone is unknown. Transport of sediment along the shear zone may occur to a greater degree than the degree of offset, such flow of sediment is thought to be coupled with fluid flow in the shear zone. High pore pressure during deformation would drive dilation or fluid/sediment flow in the shear zone. The development of a shear-zone-parallel grain fabric overprinting the other fabrics is interpreted to be a result of shear-zone-normal compaction, but to a lesser degree than in the upper splay.

Below the 440-mbsf splay, samples consist of undeformed horizontally bedded turbidites that exhibit little compaction and suggest maintenance of high pore pressure within the material during incorporation into the wedge.

Site 892

Deformation at Site 892 typically occurs as two interpenetrating conjugate fabrics formed as a bulk ductile response to out-of-sequence thrusting. Displacement indicators in the hanging wall indicate horizontal extension. This strain pattern may result either from extension associated with anticlinal folding above the thrust or extension parallel to the fault zone.

The intensity of microstructure development gradually increases downhole with proximity to the out-of-sequence thrust. Discrete deformation bands in shallow samples are discontinuous and have poor grain alignment. With depth they become wider and more continuous with a higher degree of alignment. Discontinuous kink bands with variable displacement direction are developed in several moderately deformed samples just above the 66-mbsf fault. We agree with Maltman et al.'s (1993) conclusion that these kink bands accommodate strain associated with displacement on the shear zones. The kink bands would therefore begin to form after the conjugate fabrics and continue to develop with continued displacement along the conjugate shear zones and may indicate a higher degree of strain along shear zones nearer the fault.

A minor fault is indicated above the out-of-sequence thrust by a sample containing clasts of calcite vein material. The clasts are fragmented calcite veins floating in a clayey silt matrix. Internally the clasts indicate precipitation synchronous with shear zone formation and dilation. These features indicate a repeated sequence of shearing, cataclasis, dilation, and calcite precipitation, and suggest localized fluid flow and strong interaction of fluids with faulting. The matrix fabric does not follow the trend of increasing fabric intensity and the fault is interpreted to have formed synchronously with or postdate the out-of-sequence thrust.

The out-of-sequence thrust is recognized by an interval of intense plastic deformation at 105–110 mbsf. Physical properties data for Hole 892D indicate high values of bulk density and low porosity at 105 mbsf. Porosity values are below those predicted by Brückmann's (1989) normally consolidated porosity-depth function and the background values attributed to uplift. Therefore, the effect of this deformation is enhanced consolidation. The interval contains four well-developed interpenetrating fabrics consisting of a pair of near 90° conjugate fabrics indicating plastic deformation. Displacement indicators support thrusting and band-parallel extension.

Samples collected below the out-of-sequence thrust are weakly deformed and indicate little strain. The intensity of microstructures within these samples is less than that of samples above the fault. Physical properties data also indicate higher porosity and lower bulk density below 110 mbsf. The continual increase in intensity of microstructure development above the out-of-sequence thrust suggests that the fault is responsible for generation of the trend.

Plastic deformation features associated with faults at both sites are speculated to be due to high pore pressure during deformation. While the orientation of the fault zones is consistent with Coulomb brittle failure, the shear zones themselves are deforming plastically. Such deformation requires that the internal angle of friction approach zero. Independent particulate flow of clay and silt grains occurs during plastic deformation and the internal angle of friction is effectively the sliding friction between clay and silt grains, which is speculated to decrease with elevated pore pressure.

ACKNOWLEDGMENTS

Work was supported by JOI/USSSP grants awarded to Tobin and J.C. Moore. We are grateful to the ODP drilling technicians and Shipboard Scientific Party for assistance in sample collection. We also appreciate the support, guidance, and advice of J.C. Moore. Thanks also go out to B. Tanner and J. Krupp for assistance in sample preparation.

REFERENCES

Aoki, Y., Tamano, T., and Kato, S., 1982. Detailed structure of the Nankai Trough from migrated seismic sections. *In* Watkins, J.S., and Drake, C.L. (Eds.), *Studies in Continental Margin Geology.* AAPG Mem., 34:309–322.

Arch, J., Maltman, A.J., and Knipe, R.J., 1988. Shear-zone geometries in experimentally deformed clays: the influence of water content, strain rate and primary fabric. *J. Struct. Geol.,* 10:91–99.

Bally, A.W., Gordy, P.L., and Stewart, G.A., 1966. Structure, seismic data, and orogenic evolution of the southern Canadian Rocky Mountains. *Bull. Can. Pet. Geol.,* 14:337–381.

Brückmann, W., 1989. Typische Kompakationsmuster mariner Sedimente und ihre Modifikation in einem rezenten Akkretionskeil (Barbados Ridge). *Beitr. Geol. Inst. Univ. Tübingen, Rh. A,* 5:1–135.

Byrne, T., Maltman, A., Stephenson, E., Soh, W., and Knipe, R., 1993. Deformation structures and fluid flow in the toe region of the Nankai accretionary prism. *In* Hill, I.A., Taira, A., Firth, J.V., et al., *Proc. ODP, Sci. Results,* 131: College Station, TX (Ocean Drilling Program), 83–101.

Carson, B., and Berglund, P.L., 1986. Sediment deformation and dewatering under horizontal compression: experimental results. *In* Moore, J.C. (Ed.), *Structural Fabric in Deep Sea Drilling Project Cores From Forearcs.* Mem.—Geol. Soc. Am., 166:135–150.

Dahlen, F.A., 1990. Critical taper model of fold-and-thrust belts and accretionary wedges. *Annu. Rev. Earth Planet. Sci.,* 18:55–99.

Davis, D., Suppe, J., and Dahlen, F.A., 1983. Mechanics of fold-and-thrust belts and accretionary wedges. *J. Geophys. Res.,* 88:1153–1172.

Grimm, K.A., 1992. Preparation of weakly consolidated, laminated hemipelagic sediment for high-resolution visual microanalysis: an analytical method. *In* Pisciotto, K.A., Ingle, J.C., Jr., von Breymann, M.T., Barron, J., et al., *Proc. ODP, Sci. Results,* 127/128 (Pt. 1): College Station, TX (Ocean Drilling Program), 57–62.

Hubbert, M.K., and Rubey, W.W., 1959. Role of fluid pressure in mechanics of overthrust faulting, I. Mechanics of fluid-filled porous solids and its application to overthrust faulting. *Geol. Soc. Am. Bull.,* 70:115–166.

Jim, C.Y., 1985. Impregnation of moist and dry unconsolidated clay samples using Spurr resin for microstructural studies. *J. Sediment. Petrol.,* 55:597–599.

Knipe, R.J., 1986. Faulting mechanisms in slope sediments: examples from Deep Sea Drilling Project cores. *In* Moore, J.C. (Ed.), *Structural Fabric in Deep Sea Drilling Project Cores from Forearcs.* Mem.—Geol. Soc. Am., 166:45–54.

Logan, J.M., Friedman, M., Higgs, N., Dengo, C., and Shimamoto, T., 1979. Experimental studies of simulated gouge and their application to studies of natural fault zones. *Open-File Rep.—U.S. Geol. Surv.,* 79-1239:305–343.

Lundberg, N., and Moore, J.C., 1986. Macroscopic structural features in Deep Sea Drilling Project cores from forearc regions. *In* Moore, J.C. (Ed.), *Structural Fabric in Deep Sea Drilling Project Cores From Forearcs.* Mem.—Geol. Soc. Am., 166:13–44.

Maltman, A.J., Byrne, T., Karig, D.E., Lallemant, S., Knipe, R., and Prior, D., 1993. Deformation structures at Site 808, Nankai accretionary prism, Japan. *In* Hill, I.A., Taira, A., Firth, J.V., et al., *Proc. ODP, Sci. Results,* 131: College Station, TX (Ocean Drilling Program), 123–133.

Mandl, G., 1988. *Mechanics of Tectonic Faulting: Models and Basic Concepts:* New York (Elsevier).

Mandl, G., de Jong, L.N.J., and Maltha, A., 1977. Shear zones in granular material: an experimental study of their structure and mechanical genesis. *Rock Mech.,* 9:95–144.

Moore, J.C., Brown, K.M., Horath, F., Cochrane, G., MacKay, M., and Moore, G.,1991. Plumbing accretionary prisms: effects of permeability variations. *Philos. Trans. R. Soc. London A,* 335:275–288.

Moore, J.C., and Lundberg, N., 1986. Tectonic overview of Deep Sea Drilling Project transects of forearcs. *In* Moore, J.C. (Ed.), *Structural Fabrics in Deep Sea Drilling Project Cores From Forearcs.* Mem.—Geol. Soc. Am., 166:1–12.

Moore, J.C., Moore, G.F., Cochrane, G.R., and Tobin, H.J., in press. Negative-polarity seismic reflections along faults of the Oregon accretionary prism: indicators of overpressuring. *J. Geophys. Res.*

Moore, J.C., and Vrolijk, P., 1992. Fluids in accretionary prisms. *Rev. Geophys.,* 30:113–135.

Morgenstern, N.R., and Tchalenko, J.S., 1967. Microscopic structures in kaolin subjected to direct shear. *Geotechnique,* 17:309–328.

Roeder, D., Gilbert, O.E., Jr., and Witherspoon, W.D., 1978. Evolution and macroscopic structure of Valley and Ridge thrust belt, Tennessee and Virginia. *Stud. Geol.—Tenn., Univ., Dep. Geol. Sci.,* 2.

Shipboard Scientific Party, 1994a. Site 891. *In* Westbrook, G.K., Carson, B., Musgrave, R.J., et al., *Proc. ODP, Init. Repts.,* 146 (Pt. 1): College Station, TX (Ocean Drilling Program), 241–300.

————, 1994b. Site 892. *In* Westbrook, G.K., Carson, B., Musgrave, R.J., et al., *Proc. ODP, Init. Repts.,* 146 (Pt. 1): College Station, TX (Ocean Drilling Program), 301–378.

Swartz, J.F., and Lindsley-Griffin, N., 1990. An improved impregnation technique for studying structure of unlithified cohesive sediments. *In* Suess, E., von Huene, R., et al., *Proc. ODP, Sci. Results,* 112: College Station, TX (Ocean Drilling Program), 87–91.

Tchalenko, J.S., 1968. The evolution of kink-bands and the development of compression textures in sheared clays. *Tectonophysics,* 6:159–174.

von Huene, R., 1979. Structure of the outer convergent margin off Kodiak Island, Alaska, from multichannel seismic records. *AAPG Mem.,* 29:261–272.

Westbrook, G.K., Carson, B., Musgrave, R.J., et al., 1994. *Proc. ODP, Init. Repts.,* 146 (Pt. 1): College Station, TX (Ocean Drilling Program).

White, R.S., and Louden, K.E., 1983. The Makran continental margin: structure of a thickly sedimented convergent plate boundary. *In* Watkins, J.S., and Drake, C.L. (Eds.), *Studies in Continental Margin Geology.* AAPG Mem., 34:499–518.

Date of initial receipt: 2 September 1994
Date of acceptance: 31 May 1995
Ms 146SR-251

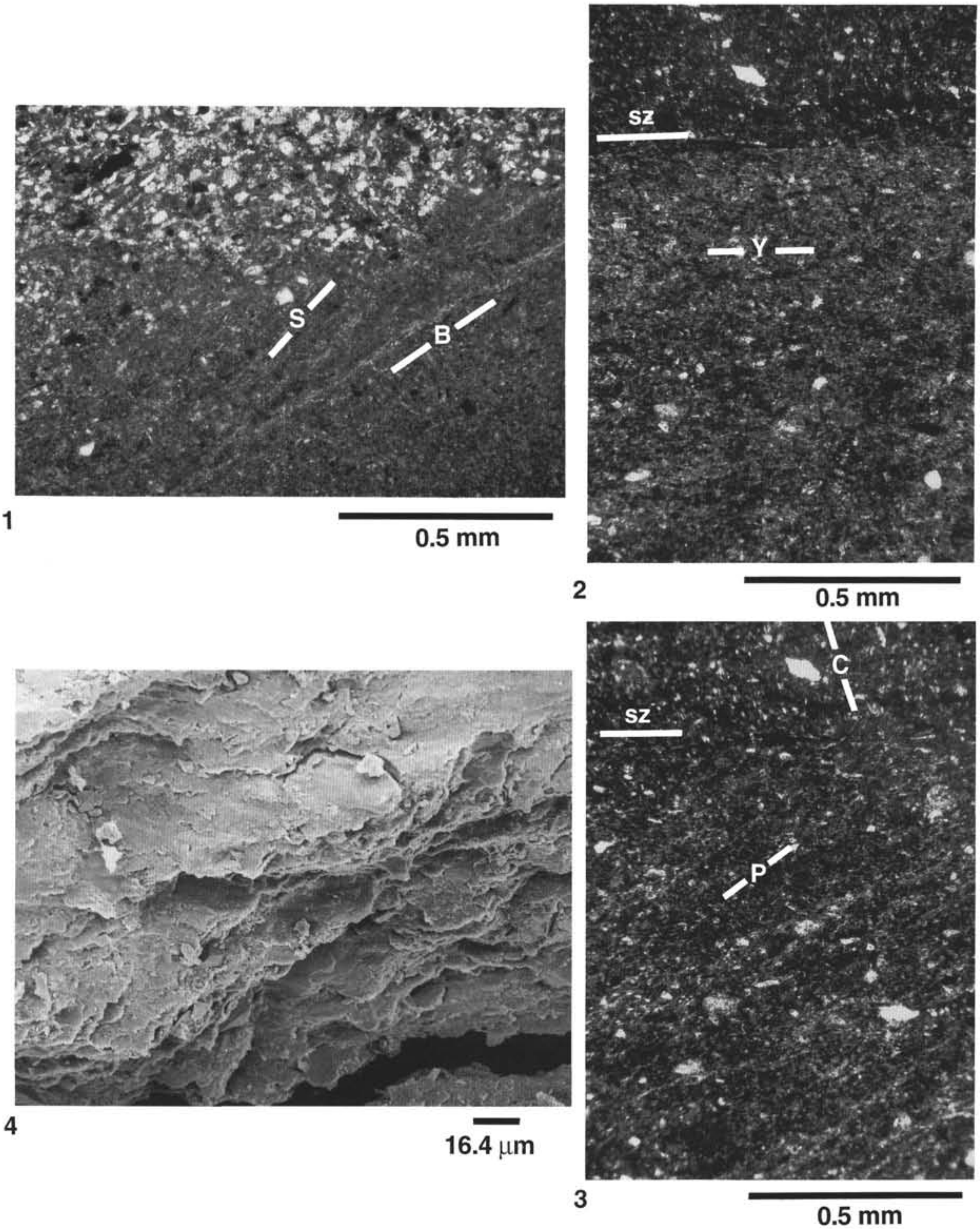

Plate 1. **1.** Sample 146-891B-30X-2, 13–26 cm. Well-developed shear zone within the uppermost clay of a turbidite sequence. Boundary shears (B) contain grains aligned parallel to the shear zone. Subsidiary shears (S) are present at a low angle to the shear zone. **2, 3, 4.** Sample 146-891B-47X-2, 92–100 cm. Wide shear zone at the upper frontal thrust splay. (2) The upper boundary of the shear zone (sz) is clearly seen, as is the well-developed Y-shear fabric (Y) defined by broad bright areas of aligned phyllosilicates. (3) 30° rotation of the thin section showing the same area as (B). Moderately developed P-shears (P) are penetrative through the shear zone. The compaction fabric (C) within material above the shear zone is at a high angle to the shear zone. (4) Subparallel sheets of aligned phyllosilicates dipping gently into the page are thought to be the Y-shear fabric (2). Grains are strongly aligned with no areas of random orientation.

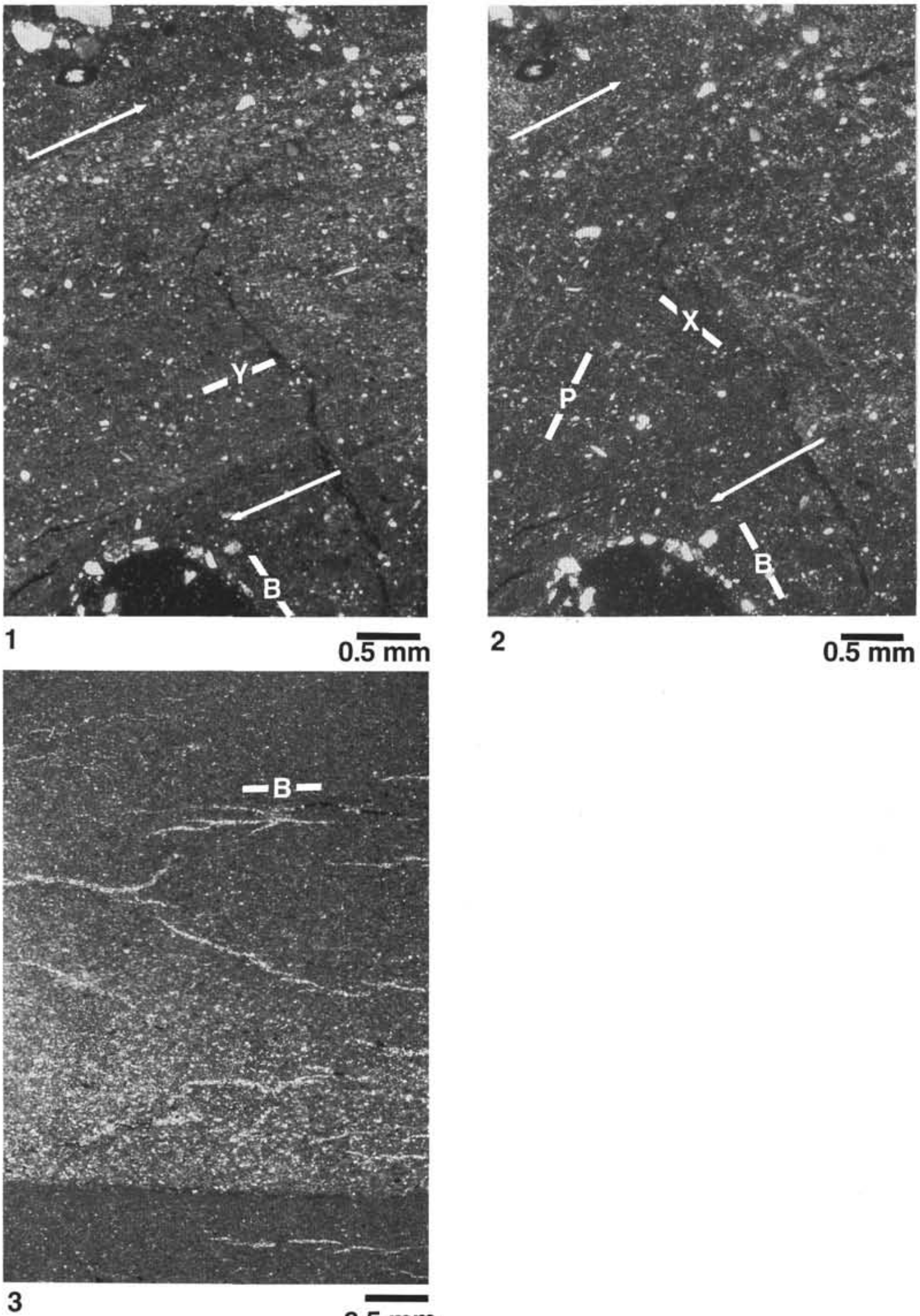

Plate 2. **1, 2.** Sample 146-891B-55X-2, 74–85 cm. Shear zone from the middle frontal thrust splay offsetting steep bedding (B), sand layers are highly plucked during preparation. The compaction fabric outside the shear zone is approximately bedding parallel. Note the lack of sand grains within the shear zone between offset bedding. (1) Distributed alignment of grains forming a Y-shear fabric (Y) indicates less strain than on the upper splay (Pl. 1, Fig. 2). (2) High-angle conjugate shears (P and X) are best illustrated at the left edge of the figure. P-shears curve and merge into the upper shear zone boundary. **3.** Sample 146-891B-58X-1, 75–95 cm. Subhorizontally bedded undeformed turbidites between the two lower frontal thrust splays show a weak compaction fabric and fissility parallel to bedding (B).

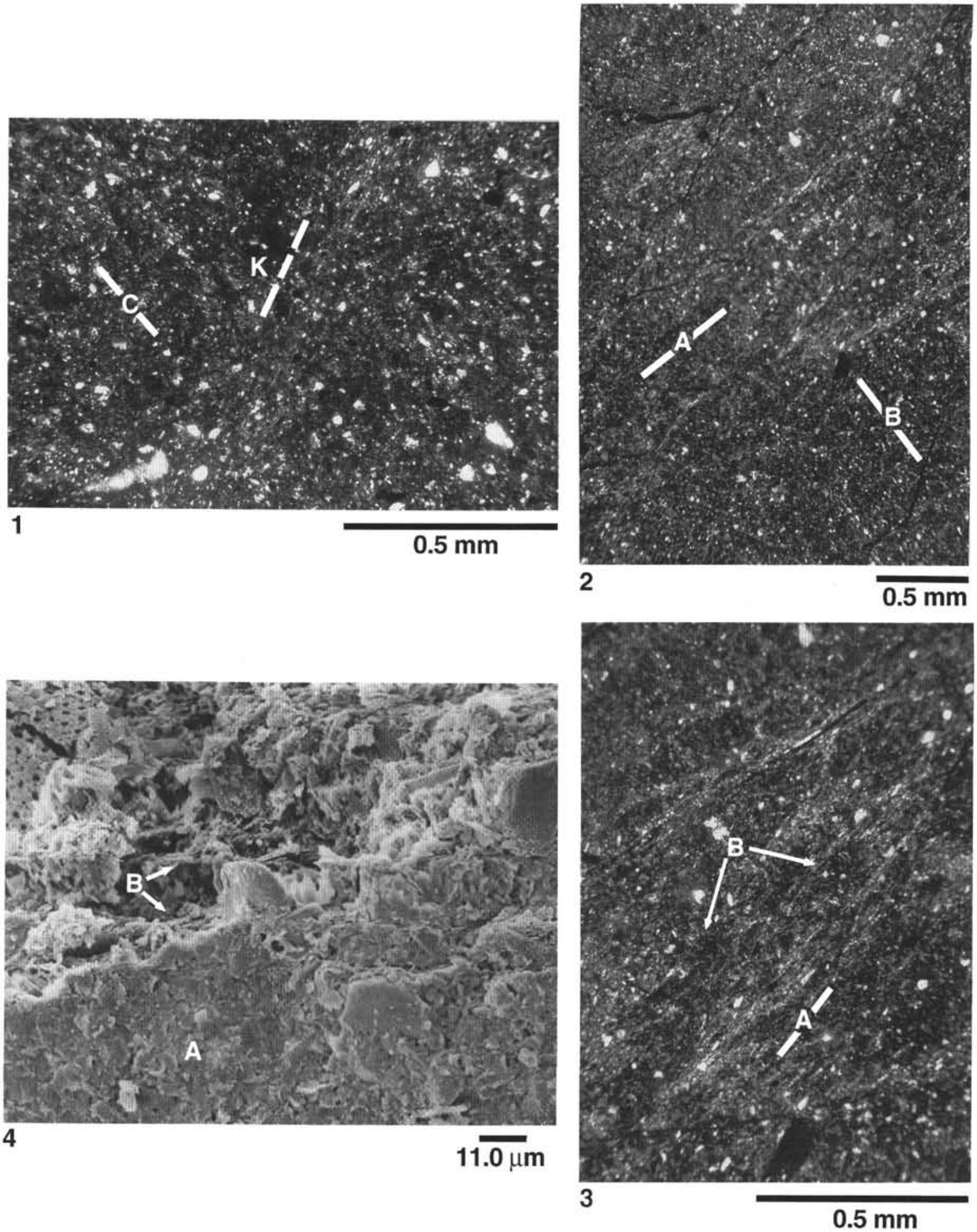

Plate 3. **1.** Sample 146-892E-4H-2, 32–36 cm. Well-developed compaction fabric (C) is cut by a high angle deformation band intermediate between kink-like and shear-like bands (K). Phyllosilicates within the kink-like band are oriented either parallel to the band or at an angle from upper right to lower left. **2, 3.** Sample 146-892E-3H-4, 116–120 cm. (2) Two fabric orientations are denoted as A and B. In this image, fabric B is defined by broad areas of alignment while fabric A is defined by both broad areas of alignment and discrete bands. This pattern reverses in other areas of the thin section. (3) Higher magnification of the central area of (2) showing grains oriented parallel to fabric B between bands of fabric A. Note the high angle between conjugate fabrics. **4.** Sample 146-892D-5X-4, 65–67 cm. In SEM fabrics are represented by planar sheets of clay grains parallel to the page (A). Grain alignment is strong but not perfect, grains appear loosely stacked. A spaced fabric (B) running left to right is defined by aligned grains and a kinking of fabric A.

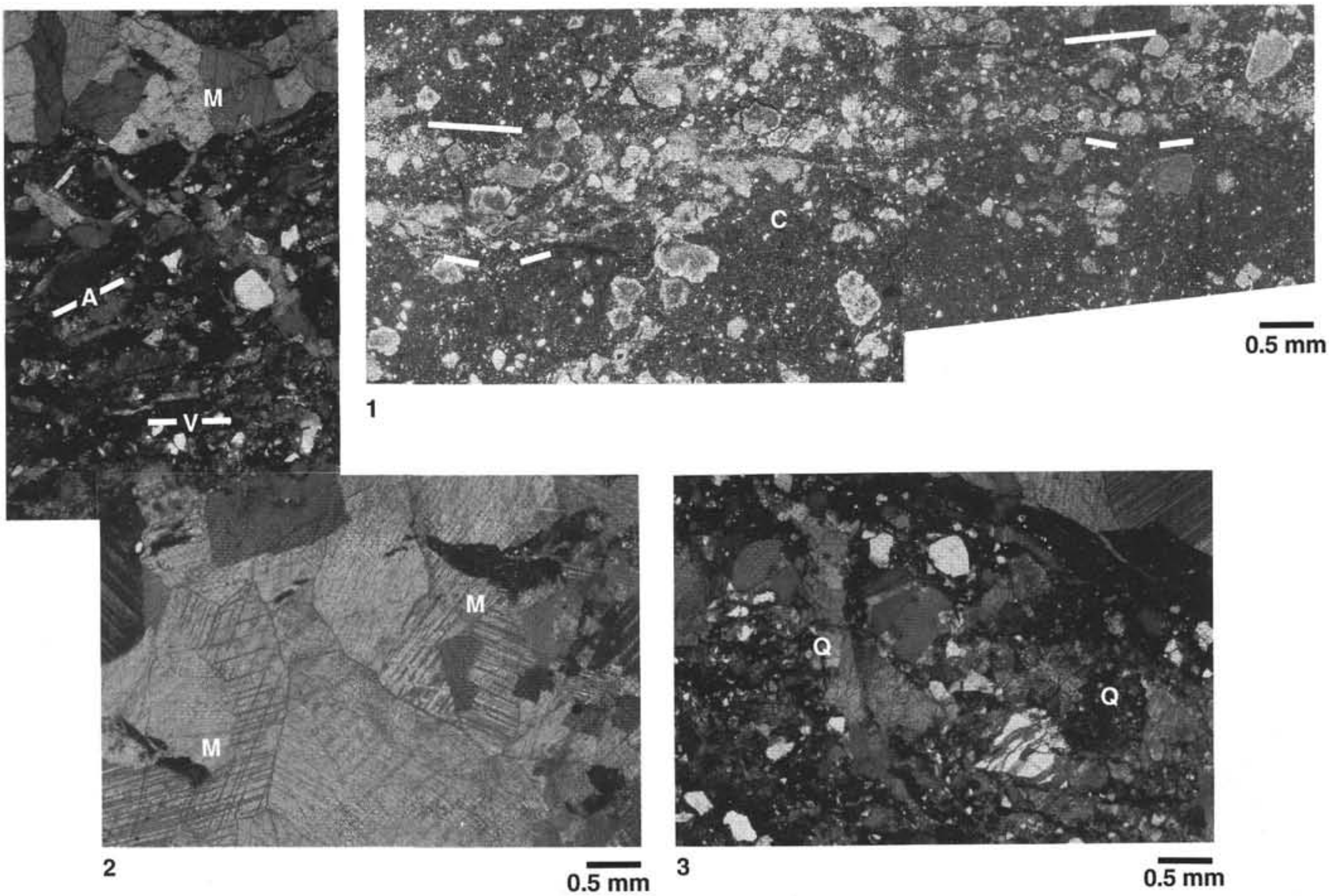

Plate 4. **1.** Sample 146-892D-6X-3, 19–22 cm. A planar to anastomosing shear zone (sz) passes from left to right through glauconite-rich sediment. Several glauconite grains have bright borders (A) in crossed polarized light, due to growth of very fine-grained alteration minerals parallel to the grain edge. Glauconite grains are also sheared out (B) along and cut by (C) the shear zone. More angular glauconite pellets occur within the shear zone and in the upper central area of the figure which is a shear splay. **2, 3.** Sample 146-892D-8X-CC, 25–28 cm. Clasts of calcite vein material within an undeformed matrix. (2) The upper and lower areas are composed of large equidimensional crystalline calcite. Clayey silt of similar composition as the matrix is incorporated within several crystals (M). In the central area, calcite, sand grains, and stringers of clayey silt are elongate at a low angle (A) to the vein orientation (V) as a result of shear during precipitation. The calcite crystals nearly perpendicular to A are only present at this location within the thin section. Inclusion of material from the sheared area within crystals at the border of the sheared calcite indicates fracture opening after shearing. (3) Quartz grains within the calcite clasts are brittlely deformed and cemented by calcite (Q).

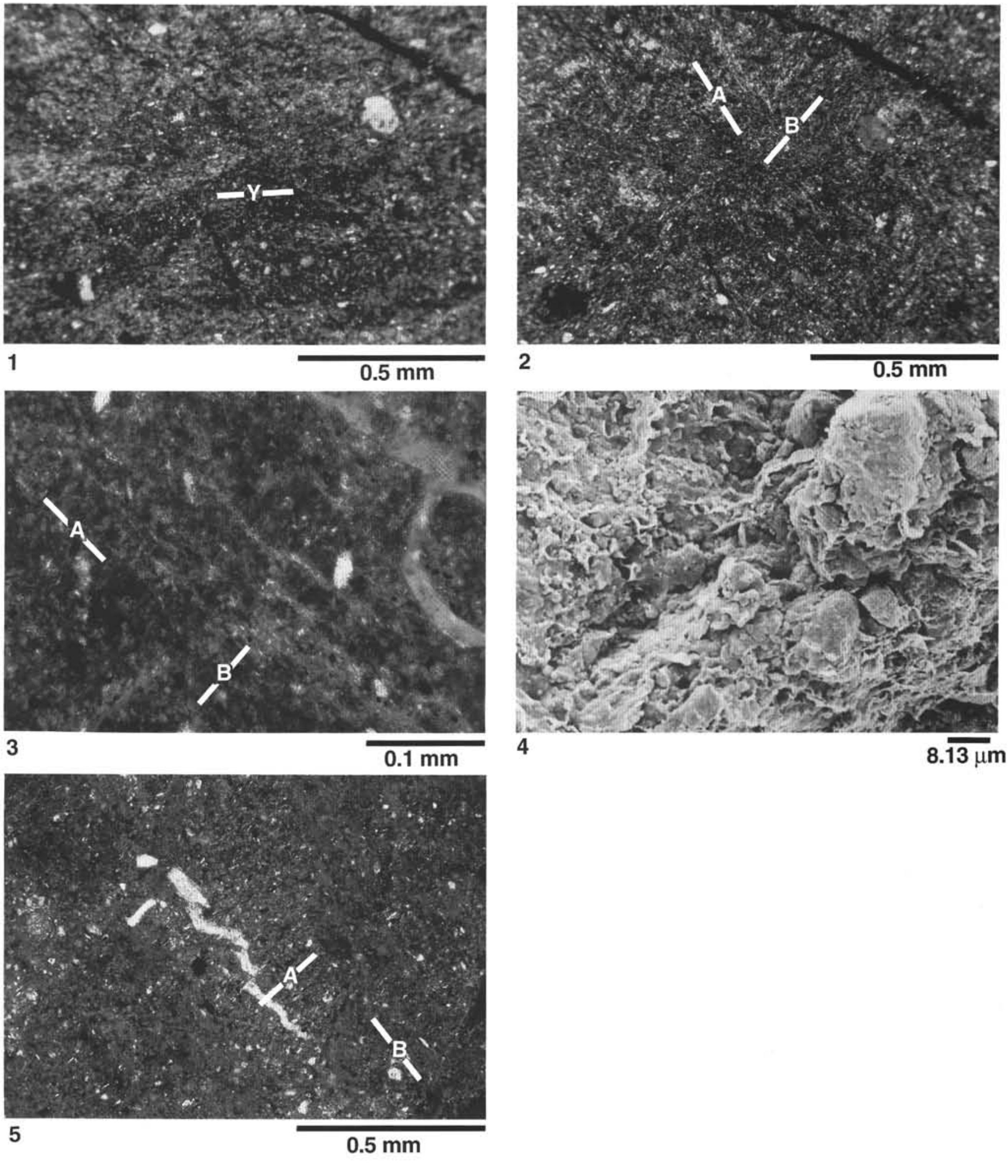

Plate 5. **1, 2.** Sample 146-892D-9X-1, 21–25 cm. Three fabric orientations are present at greater depths. (1) Broad areas of simultaneous extinction mark areas of aligned grains thought to be a moderately developed Y-shear fabric (Y). (2) 45° rotation of the thin section with the same field of view reveals a high angle conjugate set of fabrics (A and B) which are roughly bisected by the Y-shear fabric. **3.** Sample 146-892A-13X-8, 43–45 cm. At high magnification, deformation bands can be resolved into closely spaced sets of narrow bands (A) separated by material in the conjugate orientation (B). **4, 5.** Sample 146-892D-10X-3, 137–142 cm. (4) SEM images near the top of the out-of-sequence thrust indicate a relatively open framework of platy grains. Areas of preferential orientation and random alignment can be seen. Parallel alignment, however, is poor. (5) A residual clast with an internal calcite vein indicates formation after brittle fracturing of the matrix and shearing along the apparent compaction fabric. The clast is identified in the figure by the orientation of fabric within (A) and outside (B) the clast.

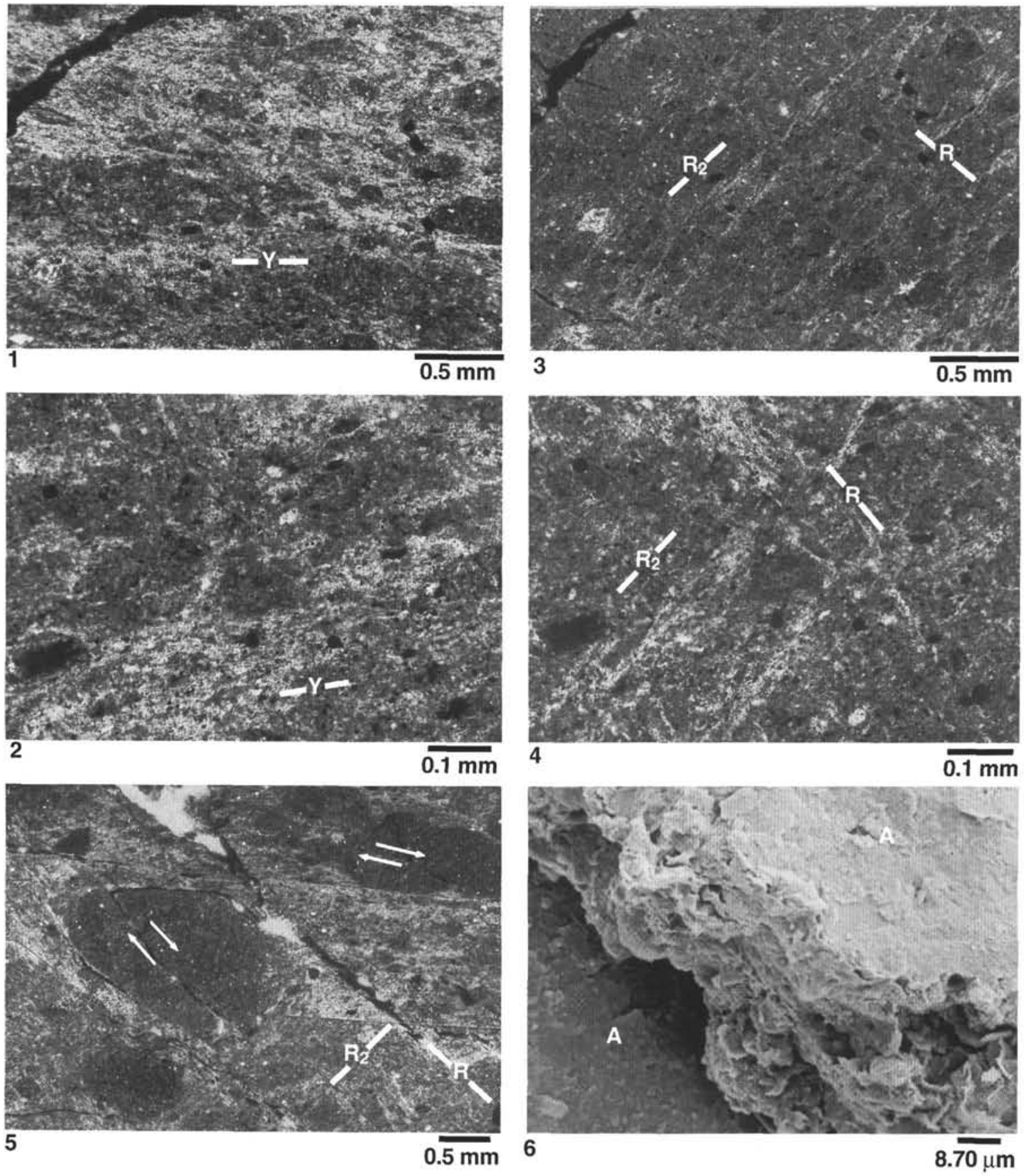

Plate 6. **1–6.** Sample 146-892D-10X-4, 124–128 cm. (1) The dominant Y-shear fabric, defined by bright areas of aligned grains (Y) and preferential alignment of elongate clasts, indicates high strain. (2) Higher magnification of the central portion of (1) showing grain alignment along Y. (3) 45° rotation of the thin section with the same field of view reveals a high angle conjugate set of fabrics R and R_2 (see Pl. 5, Fig. 5). (4) Higher magnification of the central portion of (3) showing grain alignment along these two fabrics. (5) A composite picture showing Y-shear fabric at top and R and R_2 fabrics at bottom. Residual clasts are offset right laterally along Y and R fabrics and define the sense of slip. (6) SEM images of highly deformed interval of the out-of-sequence thrust indicates parallel sheets of compressed grains (A) and a relatively open fabric between sheets.

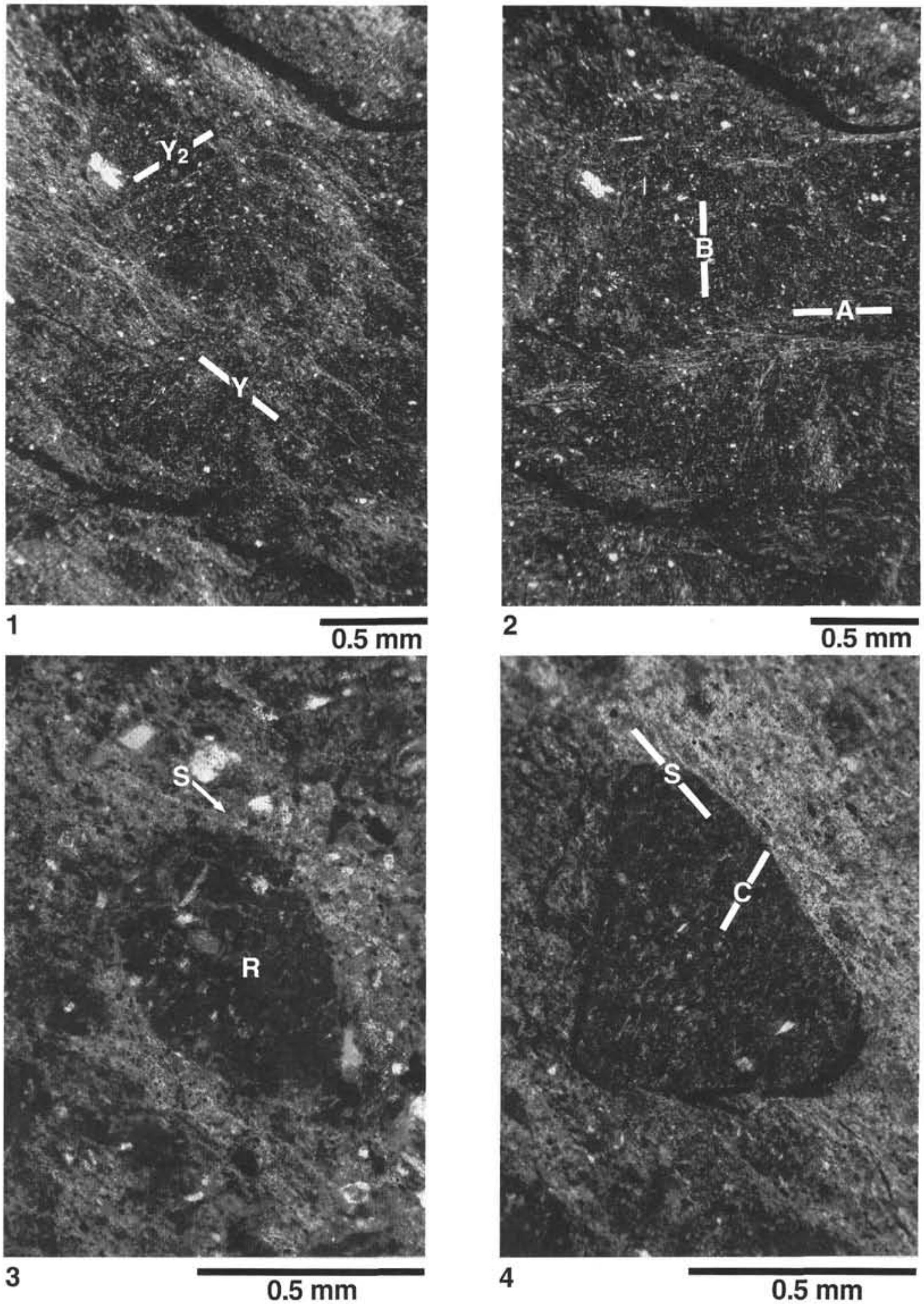

Plate 7. **1, 2.** Sample 146-892D-10X-6, 34–37 cm. (1) Samples at greater depth in Core 10X have less well developed fabrics. The Y-shear fabric (Y) consists of individual bands as well as broad areas of aligned grains. The conjugate fabric is defined by weakly developed deformation bands (Y_2) and areas of weakly aligned grains. (2) 45° rotation of the thin section with the same field of view reveals a conjugate set of fabrics which are likely R and R_2 fabrics (as in Pl. 6, Fig. 3); however, displacement indicators are absent so they are labeled A and B. **3.** Sample 146-892A-18X-1, 28–30 cm. Single strand shear zones (S) wrap around the edges of the residual clast (R), which may indicate formation as an unsheared pocket between shear bands. **4.** Sample 146-892D-10X-4, 124–128 cm. The shear fabric (S) is more commonly truncated at the clast edge. The clast's internal fabric (C) is oriented randomly with respect to external fabric, indicating clast formation prior to formation of the external fabric.